Autorotation

Invited Comment

Bohr, Jakob; Markvorsen, Steen

Published in:
Physica Scripta

Link to article, DOI:
10.1088/0031-8949/91/2/023005

Publication date:
2016

Document Version
Peer reviewed version

Revision of 17-Nov-2015

Autorotation

Jakob Bohr[1] and Steen Markvorsen[2]

[1]DTU Nanotech, Department of Micro and Nanotechnology, Building 345 East, Ørsteds Plads, Technical University of Denmark, 2800 Kongens Lyngby, Denmark, jabo@nanotech.dtu.dk

[2]DTU Compute, Department of Applied Mathematics and Computer Science, Building 303B, Technical University of Denmark, 2800 Kongens Lyngby, Denmark, stema@dtu.dk

Abstract

A continuous autorotation vector field along a framed space curve is defined, which describes the rotational progression of the frame. We obtain an exact integral for the length of the autorotation vector. This invokes the infinitesimal rotation vector of the frame progression and the unit vector field for the corresponding autorotation vector field. For closed curves we define an autorotation number whose integer value depends on the starting point of the curve. Upon curve deformations, the autorotation number is either constant, or can make a jump of (multiples of) plus-minus two, which corresponds to a change in rotation of multiples of 4π. The autorotation number is therefore not topologically conserved under all transformations. We discuss this within the context of generalised inflection points and of frame revisit points. The results may be applicable to physical systems such as polymers, proteins, and DNA. Finally, turbulence is discussed in the light of autorotation, as is the Philippine wine dance, the Dirac belt trick, and the 4π cycle of the flying snake.

Keywords

Closed space curves; Darboux vector; DNA; Dirac belt trick; Integration of generalised Frenet Serret equations; Ribbon; Signed 3D curvature.

This paper is dedicated to Ian K. Robinson on the occasion of Ian receiving the Gregori Aminoff Prize 2015.

Introduction

The combined rotation of an object that is moving along its trajectory is often an important parameter for its description. In this description the sign of the rotations are sometimes included, sometimes not. Examples of applications are diverse and include the total curvature of DNA [1], the angular motion of patients with Parkinson's disease and of spouses [2], and the difference between the length of the tropical year and the sidereal year. Presumably it is also important in the planning of new subway routes to minimise passengers discomfort as well as wear on hardware. Indeed, Piet Hein suggested the use of a super-ellipse for the geometry of a traffic roundabout at Sergels Torg in Stockholm [3]. In fluids, following the rotations of local fluid volumes may be a helpful tool for understanding flow patterns. This will be touched upon at the end of the paper, where a possible link to the phenomenon of turbulence is given.

Since the rather fortuitous discovery in 1833 of Gauss' Linking Integral, that may have followed from efforts to consolidate electromagnetism by combining Biot-Savart's law and Ampere's law, the study of the properties of space curves has been a continuing fascinating tale [4, 5] with implications in scientific disciplines, such as mathematics, physics, and molecular biology. Closed space curves exhibit various topological invariants, i.e. they are divided into sets of space curves that can be continuously transformed into each other, while curves that are topologically distinct can not. The Gauss Linking Number is known to many undergraduate physics students in disguise as the number of windings in a solenoid. For a review of the history of knot theory, see ref. [6], and for a reconstruction of Gauss' work on the linking integral, see ref. [7].

The ribbon frame

Knot equivalence is a well-known example of a concept that requires a continuous closed curve to be useful for its classification. Another well known example is the self-linking number which can be described by a continuous frame along a closed curve. Often such frames are defined from differentiable traits of the curve. Examples hereof are the Frenet Serret frame [8, 9] and the ribbon frame derived from a ribbon with Gauss curvature zero along the curve [10]. Typically, this requires $\mathcal{C}^3$ curves, and in case of the Frenet Serret frame there is a strict requirement that the curvature is nowhere vanishing. On the other hand, the ribbon frame continues smoothly where the Frenet Serret frame is discontinuous. The presence of a physical ribbon is not required as the ribbon frame is derived from the progression in space of the centre curve. The only ambiguity is a π-rotation of the frame around the tangent vector, which corresponds to a switch of choice between the two possible orientations of the ribbon surface.

The Linking number can be described as a sum of integrated twist and a double Gauss integral via the White theorem (Călugăreanu, White, Fuller) equating linking with twist plus writhe [11, 12, 13, 14]. An interesting account is given in ref. [15] where the contributions from intrinsic twist and from torsion have been separated, and the importance of the Frenet Serret frame is described. Recently, the frame of directors, also denoted the material frame, has been applied in a study of elastic ribbons and thin rods, which allows for the study of cases where the center line is not a geodesic [16].

Rotations

There are three commonly applied representations for rotations in three dimensions, namely, rotation vectors, rotation matrices, and quaternions. This includes their isomorphic representations, e.g. spinors. Representations for rotations are used interchangeably depending on ease of application, and for numerical calculation on the robustness of computations. Detailed comparison of various representations for rotations are given in refs. [17, 18] where clear and succinct tables for comparisons are presented. Rodrigues rotation formula describes the relationship between rotation vectors and rotation matrices [19, 20]. Engø's closed form [21] of the Baker-Campbell-Hausdorff formula [22, 23, 24] describes how to combine two rotation vectors. The behaviour of rotations in three-dimensional space is not always intuitive. In part, this is due to the ambiguity of rotations, e.g. whether to rotate ϕ in one direction or $2\pi - \phi$ in the opposite direction, and in part to the double covering of the rotation group SO(3) by the special unitary group SU(2), all complicated further by the non-commutative nature of rotations. Nevertheless, if one is sitting on a carousel and has been spun around four times, few would have reservations saying that they have been rotated an accumulative total of 8π.

In this paper we are studying possibilities for describing accumulative rotations from a continuous set of infinitesimal rotations in three-dimensional space, which is far less intuitive than for rotations in two-dimensions. This is equivalent to study the accumulative rotation of the frame of a framed space curve as the curve is propagated in the forward direction. We choose the rotation vector formalism as a starting point for this inquiry, and we will allow the length of the rotation vector to be unbounded.

The current investigation is also motivated by its presumed relevance for the theoretical description of polymers and biopolymers, e.g. for gaining insight into the organisation of DNA in the chromosomes and into the peculiarities of protein folding. In the description of long polymers, classical differential geometrical methods of inquiry is a successful and established field of research [25, 26]. For closed polymers, such as circular DNA, topological features such as the Linking number or knot invariants profoundly influence both statistical properties and individual molecular properties. For a detailed review of

the current understanding of topological concerns in the modeling of polymers see ref. [27].

Autorotation

By autorotation we refer to the spatial rotation of the frame of a space curve relative to the initial orientation of the frame. The understanding of the progression of such frames is an important non-trivial mathematical challenge and is related to the difficulties of integrating the Frenet Serret equations in three-dimensional Euclidean Space [28, 29, 30]. Further, as we will show, the behaviour of the autorotation vector of closed space curves can be expected to depend on topological as well as geometrical properties of the curve. We consider the case of an arbitrary frame, and in general the first frame vector does not need to be parallel with the tangent vector of the curve. When this is a requirement we will state it explicitly. Some of the results presented are dependent on having a smooth and closed frame, while the need for the curve to be closed can often be relaxed. For descriptions of the mathematics of the special case of so-called rotation-minimising-frames see refs. [31, 32, 33].

Now we introduce and define autorotation. Consider two points on a space curve $\boldsymbol{\gamma}(s)$ framed with a smooth orthogonal right handed frame $\mathcal{F}(s) = \{\mathbf{e}(s), \mathbf{f}(s), \mathbf{g}(s)\}$ and let the two points being described by the parameters $s = s_0$ and $s = s_1$. As is well known, the question of which rotation vector rotates the frame at s_0 into the frame at s_1 is ambiguous and has many answers. Let $\boldsymbol{\Omega}$ be one such rotation vector with the length ϕ and $\boldsymbol{\omega}$ a co-directional unit vector defining the axis of rotation and sign. Then the following rotation angles ϕ_{2p} also bring the two frames to superposition:

$$\phi_{2p} \in \{..., -4\pi + \phi\,, -2\pi + \phi\,, \phi\,, 2\pi + \phi\,, 4\pi + \phi\,, ...\}\ , \tag{1}$$

where the rotation vector $\boldsymbol{\Omega}_{2p} = \phi_{2p}\boldsymbol{\omega}_{2p}$ with $\boldsymbol{\omega}_{2p} = \boldsymbol{\omega}$ and $p \in \mathbb{Z}$. We can assume $\phi_{2p} \in [0 + 2p\pi, \pi + 2p\pi]$. If instead we let $-\boldsymbol{\omega}$, rather than $\boldsymbol{\omega}$, define the rotational direction then we find the additional possible rotations angles:

$$\phi_{2p+1} \in \{..., -2\pi - \phi\,, -\phi\,, 2\pi - \phi\,, 4\pi - \phi\,, 6\pi - \phi\,, ...\}\ , \tag{2}$$

where we can assume $\phi_{2p+1} \in [\pi + 2p\pi, 2\pi + 2p\pi]$, the rotation vector $\boldsymbol{\Omega}_{2p+1} = \phi_{2p+1}\boldsymbol{\omega}_{2p+1}$ with $\boldsymbol{\omega}_{2p+1} = -\boldsymbol{\omega}$. Now the autorotation can be defined as follows,

Definition 1: The autorotation angle, ϕ_A, the autorotation unit field vector, $\boldsymbol{\omega}_A$, and the autorotation vector, $\boldsymbol{\Omega}_A$, for the frame field, $\mathcal{F}$, are defined by the requirements a) through e):

a) ϕ_A is a possible rotation angle, see lists above.
b) $\boldsymbol{\omega}_A$ is a unit vector along the axis of rotation.
c) $\boldsymbol{\Omega}_A = \phi_A \boldsymbol{\omega}_A$.
d) Up to a sign, the ambiguity in ϕ is lifted by the requirements that $\phi_A = 0$ for $s = s_0$ and that $\boldsymbol{\Omega}_A$, $\boldsymbol{\omega}_A$, and ϕ_A are all varying smoothly with the curve parameter, s.
e) The final sign ambiguity is lifted by the requirement that $\phi_A(s_0 + \epsilon) > 0$ where $\epsilon > 0$ and infinitesimal small.

A short example of the autorotation vector, $\boldsymbol{\Omega}_A$, is given in Figure 1 with the corresponding autorotation angle, ϕ_A, shown in Figure 2. Notice that the particular sign convention in e) is a choice. The disadvantage of this choice is that the definition now depends on a local properties of $\mathcal{F}$. The advantage is that it removes the ambiguity in the definition of the autorotation number. As can be seen, the frame at s_0 defines the reference points from which the progression of the rotation is mapped; in the following s_0 is assumed to be zero if not stated otherwise. From the requirement that the autorotation angle, ϕ_A, and unit vector $\boldsymbol{\omega}$ both vary smoothly it follows that ϕ_A can not jump between the discrete rotations enumerated in (1) and (2). The cases when ϕ is a integer multiple of π will be discussed later in the text.

Rodrigues' rotation vector

In the following we are interested in tracking how the rotation of a moving frame propagates as one moves along a curve $\boldsymbol{\gamma}(s)$. We will consider an orthogonal right handed frame consisting of three unit vector fields along the oriented curve $\boldsymbol{\gamma}(s)$ with a unit speed parametrisation given by s

$$\{\mathbf{e}(s), \mathbf{f}(s), \mathbf{g}(s)\} \tag{3}$$

Now let $\mathbf{R}(s_1, s_2)$ be the rotation matrix defined by the equation

$$(\mathbf{e}(s_2), \mathbf{f}(s_2), \mathbf{g}(s_2)) = (\mathbf{e}(s_1), \mathbf{f}(s_1), \mathbf{g}(s_1))\mathbf{R}^T(s_1, s_2) \ , \tag{4}$$

where the superscript ^{T} refers to transposition. The rotation, given by the matrix $\mathbf{R}(s_1, s_2)$, is equivalently described by a rotation vector $\boldsymbol{\Omega}(s_1, s_2)$, with a directional unit vector $\boldsymbol{\omega}(s_1, s_2)$ along the axis of rotation and $\phi(s_1, s_2)$ equal to the angle of rotation, i.e. with $\boldsymbol{\Omega}(s_1, s_2) = \phi(s_1, s_2)\, \boldsymbol{\omega}(s_1, s_2)$. The Rodrigues rotation formula describes the relation between the rotation matrix $\mathbf{R}(s_1, s_2)$ and the rotation vector $\boldsymbol{\Omega}(s_1, s_2)$ as

$$\mathbf{R}\mathbf{v} = \mathbf{v} + \sin\phi\, \boldsymbol{\omega} \times \mathbf{v} + (1 - \cos\phi)\, \boldsymbol{\omega} \times \boldsymbol{\omega} \times \mathbf{v} \ , \tag{5}$$

where s_1 and s_2 are not explicitly stated, and $\mathbf{v}$ is any vector being rotated [19, 20]. The rotation vector, $\boldsymbol{\Omega} = \phi\, \boldsymbol{\omega}$, is sometimes called the Rodrigues vector. There is a

corresponding skew matrix notation, $\widetilde{\mathbf{\Omega}}(s_1, s_2)$ that can be used interchangeably with the Rodrigues vector description $\mathbf{\Omega}$ depending on which of the two is the more convenient for the purpose at hand. For the skew matrix notation the Rodrigues rotation formula becomes [20]

$$\mathbf{R} = \mathbf{E} + \sin\phi\,\widetilde{\boldsymbol{\omega}} + (1 - \cos\phi)\,\widetilde{\boldsymbol{\omega}}^2 \ , \tag{6}$$

where $\phi\,\widetilde{\boldsymbol{\omega}} = \widetilde{\mathbf{\Omega}}$ and $\mathbf{E}$ is the 3×3 identity matrix. Equation (6) is equivalent to $\mathbf{R} = \exp(\widetilde{\mathbf{\Omega}})$ where exp is the corresponding exponential map of matrices.

Infinitesimal rotation vector

The following notation will be used,

$$\mathbf{R}(s, s + \Delta s) = \mathbf{E} + \widetilde{\mathbf{D}}(s)\Delta s + O(\Delta s^2) \ , \tag{7}$$

and

$$\mathbf{R}(0, s + \Delta s) = \mathbf{R}(s, s + \Delta)\mathbf{R}(0, s) \ , \tag{8}$$

where $\widetilde{\mathbf{D}}$ is the skew symmetric infinitesimal rotation matrix, consequently found as

$$\widetilde{\mathbf{D}}(s) = \dot{\mathbf{R}}(0, s)\mathbf{R}^T(0, s) \ . \tag{9}$$

where the dot above $\mathbf{R}(0, s)$ indicates differentiation with respect to s. To the skew symmetric matrix $\widetilde{\mathbf{D}}$ there is a corresponding infinitesimal rotation, $\mathbf{D}$, for which one has $\mathbf{R}(s, s + \Delta s)\mathbf{v} = \mathbf{v} + \Delta s\,\mathbf{D}(s) \times \mathbf{v} + O(\Delta s^2)$. For studies of Frenet Serret frames [34], as well as for ribbon frames with Gauss curvature zero [10], the infinitesimal rotation vector $\mathbf{D}$ becomes the classical Darboux vector.

A short note of caution with regards to the use of the greek letter omega. In the literature omega has various uses including that as angular velocity and that as a unit rotation vector. In this paper $\boldsymbol{\omega}$ is a unit vector indicating the axis of rotation. The infinitesimal rotation vector $\mathbf{D}$ corresponds to the angular velocity of the frame of unit speed curves.

Decomposition of the infinitesimal rotation

The purpose of this section is to detail the relationship between the sequential application of a continuum set of infinitesimal rotations and the resulting macroscopic rotation relative to $\mathcal{F}(s_0)$. By direct differentiation of the Rodrigues rotation formula (5) we obtain the following theorem for the relationship between a global rotation vector $\mathbf{\Omega}$ and the

continuous set of underlying local infinitesimal rotation vector field $\mathbf{D}$.

Theorem 1: We let $\mathbf{R}(s)$ denote a smooth 1-parameter family of rotation matrices parameterised by s. The associated Rodrigues vector (w.r.t. any fixed orthogonal frame) is denoted by $\mathbf{\Omega}(s) = \phi(s)\boldsymbol{\omega}(s)$ with unit vector $\boldsymbol{\omega}(s)$ and rotation angle $\phi(s)$. The infinitesimal rotation vector associated with $\mathbf{R}(s)$ is denoted by $\mathbf{D}(s)$ and here called the generalised Darboux vector.

We have the following decomposition of the generalised Darboux vector:

$$\mathbf{D}(s) = \dot{\phi}(s)\boldsymbol{\omega}(s) + \sin(\phi(s))\dot{\boldsymbol{\omega}}(s) + (1 - \cos(\phi(s)))\boldsymbol{\omega}(s) \times \dot{\boldsymbol{\omega}}(s) \ . \tag{10}$$

Assuming that $\dot{\boldsymbol{\omega}}(s) \neq \mathbf{0}$ we let $\{\mathbf{a}(s), \mathbf{b}(s), \mathbf{c}(s)\}$ denote the following orthonormal *frame:*

$$\begin{aligned} \mathbf{a}(s) &= \boldsymbol{\omega}(s) \\ \mathbf{b}(s) &= \frac{\dot{\boldsymbol{\omega}}(s)}{\|\dot{\boldsymbol{\omega}}(s)\|} \\ \mathbf{c}(s) &= \mathbf{a}(s) \times \mathbf{b}(s) \end{aligned} \tag{11}$$

Then we have the following equivalent decomposition of $\mathbf{D}(s)$ w.r.t. that frame:

$$\mathbf{D}(s) = \dot{\phi}(s)\mathbf{a}(s) + 2\,\|\dot{\boldsymbol{\omega}}(s)\|\,\sin\left(\frac{\phi(s)}{2}\right)\left(\cos\left(\frac{\phi(s)}{2}\right)\mathbf{b}(s) + \sin\left(\frac{\phi(s)}{2}\right)\mathbf{c}(s)\right) \ . \tag{12}$$

Perhaps a quaternion analysis will provide the most brief exposition hereof:

Proof: The Rodrigues rotation vector $\mathbf{\Omega}(s) = \phi(s)\boldsymbol{\omega}(s)$ corresponds to the equivalent quaternion:

$$\begin{aligned} \mathbf{Q}_{\Omega(s)} &= \cos(\phi(s)/2) + \sin(\phi(s)/2)(\omega_1(s)\mathbf{i} + \omega_2(s)\mathbf{j} + \omega_3(s)\mathbf{k}) \\ &= (\,\cos(\phi(s)/2)\,,\ \sin(\phi(s)/2)\boldsymbol{\omega}(s)) \end{aligned} \tag{13}$$

we have used the shorthand notation for the quaternions $\mathbf{Q} = (s, \mathbf{v})$ for which the quaternion product conveniently becomes

$$\mathbf{Q}_1 \odot \mathbf{Q}_2 = (s_1 s_2 - \mathbf{v}_1 \cdot \mathbf{v}_2\,,\ s_1\mathbf{v}_2 + s_2\mathbf{v}_1 + \mathbf{v}_1 \times \mathbf{v}_2) \tag{14}$$

The skew symmetric matrix which is equivalent to the Darboux vector is denoted by $\widetilde{\mathbf{D}}(s)$ and given by equation (9) above. The corresponding quaternion describing this infinitesimal rotation is [18, 35]

$$\mathbf{Q}_{\widetilde{D}(s)} = 2\dot{\mathbf{Q}}_{\Omega(s)} \odot \mathbf{Q}^{\dagger}_{\Omega(s)} \quad , \tag{15}$$

where $\mathbf{Q}^{\dagger}_{\Omega(s)}$ *is the quaternian conjugate of* $\mathbf{Q}_{\Omega(s)}$*:*

$$\mathbf{Q}^{\dagger}_{\Omega(s)} = (\cos(\phi(s)/2)\,,\ -\sin(\phi(s)/2)\boldsymbol{\omega}(s)) \quad . \tag{16}$$

Interestingly, this completes the proof for the formula (eq. 10) for the decomposition of $\mathbf{D}(s)$*:*

$$\begin{aligned} \mathbf{Q}_{\widetilde{D}(s)} &= 2\dot{\mathbf{Q}}_{\Omega(s)} \odot \mathbf{Q}^{\dagger}_{\Omega(s)} \\ &= \Big(0,\ \dot{\phi}(s)\boldsymbol{\omega}(s) + \sin(\phi(s))\dot{\boldsymbol{\omega}}(s) + (1-\cos(\phi(s)))\boldsymbol{\omega}(s)\times\dot{\boldsymbol{\omega}}(s)\Big) \\ &= (\,0,\ \mathbf{D}(s)) \quad . \end{aligned} \tag{17}$$

We may now state the associated corollary.

Corollary 1: In particular we have that

$$\begin{aligned} \boldsymbol{\omega}(s)\cdot\mathbf{D}(s) &= \dot{\phi}(s) \\ \dot{\boldsymbol{\omega}}(s)\cdot\mathbf{D}(s) &= \|\dot{\boldsymbol{\omega}}(s)\|^2\,\sin(\phi(s)) \\ (\boldsymbol{\omega}(s)\times\dot{\boldsymbol{\omega}}(s))\cdot\mathbf{D}(s) &= \|\dot{\boldsymbol{\omega}}(s)\|^2\,(1-\cos(\phi(s)))\ . \end{aligned} \tag{18}$$

With $\dot{\boldsymbol{\Omega}} = \dot{\phi}\boldsymbol{\omega}_V + \phi\dot{\boldsymbol{\omega}}_V$ we can formally integrate and obtain an expression for $\boldsymbol{\Omega}(0,s)$. Subsequently, one can apply Rodrigues rotation formula and obtain the forward transport of the first frame vector. If the first frame vector is taken as the tangent vector then its integration gives directly the corresponding space curve parameterisation. Thus, in principle one can obtain a condition for a space curve to be closed, see also the discussion in ref. [36].

Uniqueness and existence

In this section we wish to comment on the autorotation angle, ϕ_A in details. The equations, especially (10) and (18), are applicable to the global autorotation fields ($\boldsymbol{\Omega}_{\mathbf{A}}$, ϕ_A, and $\boldsymbol{\omega}_A$). Consider the ϕ solutions earlier stated in equation (1) and (2): what happens at those of the integer multiples of π points where a jump from one solution ϕ to a neighbouring solution is required. By a double sign inversion in equation (2) both ϕ and $\boldsymbol{\omega}$ can be smoothly continued.

The double change in sign between one π-interval to the next which followed directly from equations (1) and (2) also secures the uniqueness of the continuation for so far that a smooth continuation exists. The reason being that a continuation in the neighbouring π-interval and a continuation staying within one and the same π-interval can not both have a smooth continuation of the unit rotation vector field $\boldsymbol{\omega}$. I.e. whether or not a shift to a neighbouring solution is done depends on which choice gives a smooth continuation of the autorotation field. Since the uniqueness is secured we shall now visit the question of condition for existence.

With the initial reference at s_1 the autorotation angle at s_2 can be found as the following integral

$$\phi_A(s_1, s_2) = \int_{s_1}^{s_2} \dot{\phi}_A(s_1, s)\, ds = \int_{s_1}^{s_2} \boldsymbol{\omega}_A(s_1, s) \cdot \mathbf{D}(s)\, ds \ . \tag{19}$$

As mentioned above special considerations are required for obtaining the proper smooth continuous autorotation angle, ϕ_A, at the points where $\phi = q\pi$ where $q \in \mathbb{Z}$.

When $\phi_A = q\pi$, $q \in \mathbb{Z}$ at a point given by $s = s_3$ then the unit autorotation vector $\boldsymbol{\omega}_A(s_3)$ is *per se* well defined by the requirement of smoothness, i.e.

$$\boldsymbol{\omega}_A(s_3) = \lim_{s \to s_3^-} \boldsymbol{\omega}_A(s) \ . \tag{20}$$

The questions of how to continue the autorotations fields requires considerations of various scenarios. The case for which $\dot{\phi}(s_3) \neq 0$ is simple as the continuation is straight forward. The autorotation angle continues to increase (or decrease) and thereby moves in to the neighbouring π-interval. Less obvious is the choice when $\dot{\phi}(s_3) = 0$, which can also be seen from reconsidering Equation (10) and the need for including the first non-vanishing term of the Taylor expansion. At first sight, the derivative of the autorotation angle can become zero if either

a) $\mathbf{D} = \mathbf{0}$,

b) $\boldsymbol{\omega} \perp \mathbf{D}$.

This leaves three cases, a), b), or a) $\wedge$ b) to be investigated further. In short, one needs to decide whether the resulting action is a continuing accumulation (or depletion) of the autorotation angle, or a local extremum. This corresponds to considering whether the first non-vanishing power of the corresponding Taylor expansion is odd or even (assumed finite). A single criterion which embodies all situations can be stated using the autorotation parity defined here,

Definition 2: *The autorotation parity, $\sigma_\phi(s)$, for a smooth framed three dimensional space*

curve $\boldsymbol{\gamma}(s)$ is defined as

$$\sigma_\phi(s) = \lim_{\epsilon \to 0} \left(\frac{\boldsymbol{\omega}(s) \cdot \mathbf{D}(s-\epsilon)}{|\boldsymbol{\omega}(s) \cdot \mathbf{D}(s-\epsilon)|} \frac{\boldsymbol{\omega}(s) \cdot \mathbf{D}(s+\epsilon)}{|\boldsymbol{\omega}(s) \cdot \mathbf{D}(s+\epsilon)|} \right) \quad , \tag{21}$$

where $\mathbf{D}(s)$ is the generalised Darboux vector associated with $\boldsymbol{\gamma}(s)$. The unit autorotation vector is $\boldsymbol{\omega}(s)$ where the reference point s_0 is not explicitly shown.

With reference to equations (10) and (18) we have $\dot{\phi}(s) = \boldsymbol{\omega}(s) \cdot \mathbf{D}(s)$ and hence the following lemma.

Lemma 1: *A sufficient and necessary criterion for the autorotation angle, $\phi(s)$, to have an extrema is that the autorotation parity, $\sigma_\phi(s)$, is minus one, i.e. $\sigma_\phi(s) = -1$.*

It is worthwhile with a short digression into the regular geometrical inflections points of curves. Let's first consider planar two-dimensional curves, we can determine the inflection points as the points where the following curvature parity is minus one.

Definition 3: The total curvature parity, σ_K of a smooth two-dimensional curve is defined as

$$\sigma_K(s) = \lim_{\epsilon \to 0} \left(\frac{\kappa(s-\epsilon)}{|\kappa(s-\epsilon)|} \frac{\kappa(s+\epsilon)}{|\kappa(s+\epsilon)|} \right) \quad , \tag{22}$$

where the subscript refers to the total signed curvature $K(s)$. Its derivative, $\dot{K}(s)$, is the conventionally defined signed curvature, $\kappa(s)$, for two-dimensional curves.

For a planar curve dressed with a ribbon frame (a ribbon with Gauss curvature zero) both of the vectors $\mathbf{D}$ and $\boldsymbol{\omega}$ are perpendicular to the plane of the curve and it follows straight forwardly that $\sigma_K(s) = \sigma_\phi(s)$. The inflection points of the planar curve are found at the points where $\sigma_K(s) = -1$, which indicates the points where the total signed curvature has an extrema.

3D signed curvature and inflection points

Let us now consider regular inflection points of three-dimensional space curves. There are slight variations of their definition in the literature. Here we will proceed as follows. Along a three-dimensional space curve it is possible to define a signed curvature, κ_{3D}, up to a single sign ambiguity which will invert the numbers consistently along the entire curve. This idea of a signed curvature has been promoted by various authors, e.g. Nomizu [37] and Bates & Melko [38]. Further, it was noticed that a signed curvature for space curves appears naturally from the parameterisation of the ribbon frame [10]. We can now define

a parity, $\sigma_{K_{3D}}$, by extending definition 3 to the three-dimensional case. Notice that the sign ambiguity is properly canceled by the parity definition. In the following, we will use the same notation σ_K for both the two and the three-dimensional case, and we will define the geometrical inflection points of a smooth space curve to be exactly the points where $\sigma_K = -1$.

The ribbon frame referred to earlier in the text and in ref. [10] is characterised by being associated with a ribbon having Gauss curvature zero everywhere. The ribbon frame $(\mathbf{e}(s), \mathbf{f}(s), \mathbf{g}(s))$ coincidence with the Frenet Serret frame $(\mathbf{t}(s), \mathbf{n}(s), \mathbf{b}(s))$ on parts of the curve, here $\mathbf{t}(s)$ is the tangent vector, $\mathbf{n}(s)$ the normal vector, and $\mathbf{b}(s)$ the binormal vector. On other parts of the curve the second and third frame vector is inverted, i.e. $(\mathbf{e}(s), \mathbf{f}(s), \mathbf{g}(s))$=$(\mathbf{e}(s), -\mathbf{f}(s), -\mathbf{g}(s))$. Importantly, the ribbon frame is well defined at the points where the Frenet Serret frame is not. Therefore, the ribbon frame provides a convenient tool for the location of the inflection points of a smooth three-dimensional space curve. These geometrical inflection points can be determined from the curvature parity defined below.

Definition 4: The total signed curvature parity, σ_K, of a smooth three-dimensional space curve $\boldsymbol{\gamma}(s)$ is defined as

$$\sigma_K(s) = \lim_{\epsilon \to 0} \left(\frac{\mathbf{g}(s) \cdot \mathbf{D}(s-\epsilon)}{|\mathbf{g}(s) \cdot \mathbf{D}(s-\epsilon)|} \frac{\mathbf{g}(s) \cdot \mathbf{D}(s+\epsilon)}{|\mathbf{g}(s) \cdot \mathbf{D}(s+\epsilon)|} \right) \quad , \tag{23}$$

where $\mathbf{g}(s)$ is the second frame vector of the intrinsically flat ribbon frame and $\mathbf{D}(s)$ is the corresponding classical Darboux vector for which the length is given by the curvature and torsion as $\sqrt{\kappa^2 + \tau^2}$.

Here it has been utilised that the infinitesimal rotation vector for the ribbon frame $\mathbf{D} = \tau\mathbf{e} + \kappa\mathbf{g}$ is equal to the classical Darboux vector $\mathbf{D} = \tau\mathbf{t} + |\kappa|\mathbf{b}$ where κ is the signed 3D curvature. Similarly to the determination of the inflection points from the criterion $\sigma_K = -1$, one can keep track of the extrema by $\sigma_K = +1$. For curiosity it is worthwhile to notice that the extrema of the total torsion can be found using a correspondingly defined parity.

Definition 5: The total torsion parity, σ_T, of a smooth three dimensional space curve $\boldsymbol{\gamma}(s)$ is defined as

$$\sigma_T(s) = \lim_{\epsilon \to 0} \left(\frac{\mathbf{e}(s) \cdot \mathbf{D}(s-\epsilon)}{|\mathbf{e}(s) \cdot \mathbf{D}(s-\epsilon)|} \frac{\mathbf{e}(s) \cdot \mathbf{D}(s+\epsilon)}{|\mathbf{e}(s) \cdot \mathbf{D}(s+\epsilon)|} \right) \quad , \tag{24}$$

where $\mathbf{e}(s)$ is the tangent vector and $\mathbf{D}(s)$ is the classical Darboux vector.

Closed Space Curves

Consider a closed space curve with $s \in [0, L]$ with a continuous ribbon frame for which $\mathbf{e}(L) = \mathbf{e}(0)$, and similarly for $\mathbf{f}$ and $\mathbf{g}$, and for which the curve and the frame repeat themselves smoothly modulo L. It then follows that the total signed curvature is a smooth function and that $\kappa(0) = \kappa(L)$. Recall that the signed curvature is determined up to a single choice of sign. A convenient choice is to let the sign be determined by s_0 such that $\kappa(s_{0+}) > 0$. As the derivative of the total curvature is cyclic with the period L, it consequently must have an even number of extrema.

Lemma 2: The total number of geometrical inflection points on a smooth closed three-dimensional space curve with a continuous ribbon frame is either zero or a positive even number.

This statement regarding the geometrical inflection points is closely related to the findings of Randrup and Røgen [39] on frame switching points of the Frenet Serret frame as there is a one-to-one match with the inflection points of the curve. A Möbius strip will have an odd number of inflection points as it needs to be traversed twice for a smooth closure of the ribbon frame. Note that the solution with no inversion points is not valid as in this case one has $\kappa(L+s) = -\kappa(s)$ for the signed curvature. See also the discussions in [39, 40] including the account of a discontinuity in the curvature in the limit when the width of the Möbius strip is null [40]. Inflection points are also important for the statistical mechanics of developable ribbons [41, 42] and has been linked to disequilibrium of magnetic flux-tubes [43].

The autorotation number

For a closed space curve with a continuous and smooth framing it is assumed that the curve and the frame repeats itself smoothly modulo L. The autorotation $\phi_A(s_0, s_0 + L)$ must therefore be an integer m times 2π where $m \in \mathbb{Z}$ as the initial frame and the end frame are revisits of the same frame. The previously mentioned dependence of the integer autorotation $m(s_0)$ on s_0 will be investigated in the following,

Definition 6: The autorotation number, $m \in \mathbb{Z}$, of a closed framed space curve is the integer number of 2π's which equals to the length of the autorotation vector corresponding to one full progression of the curve. It is measured using the smooth propagation of the frame starting from a reference frame s_0:

$$m(s_0) = \frac{||\mathbf{\Omega}_A(s_0, s_0 + L)||}{2\pi} = \frac{\phi_A(s_0, s_0 + L)}{2\pi} \quad . \tag{25}$$

In general, the autorotation number behaves nicely and does not depend on the choice of initial point within an interval around s_0. There are some exceptions. Firstly, with respect to the initial point:

Lemma 3: The autorotation number changes sign when the choice of the initial point passes through a point where the total curvature parity, σ_K, is minus one.

This dependence on the initial point is a simple consequence of the way we have chosen to define the initial direction of the unit autorotation vector field. It is natural to ask what happens with m when one perturbs the framed curve either through some local move or global moves which preserve the topology. For local moves, the autorotation number, m, is preserved. This follows from its integer nature and its differential construction. However, m will generally not be conserved for moves where the $\sigma_\phi = -1$ points are reconfigured globally. A helpful concept in the discussion is that of frame revisits. From the definition of the autorotation number a peculiar result that is valid for specific closed space curves can be directly stated:

Lemma 4: For closed space curves for which m is 2, or greater, the initial frame of the space curve is repeated at least m-1 times along the curve.

It follows straightforwardly from the continuity of the vector field $\mathbf{\Omega}_A(s_0, s)$ where $s \in [s_0, L + s_0]$ that there must be at least one value of $s \neq s_0$ for which $||\mathbf{\Omega}_A(s_0, s)|| = 2\pi$, and so forth.

By integration of $\dot{\phi}_A = \boldsymbol{\omega}_A(s)\cdot\mathbf{D}(s)$ one can now obtain the following autorotation theorem for a closed space curve,

Theorem 2: For a closed space curve with a differential frame the curve integral of the projection of the infinitesimal rotation vector on the direction of the instantaneous accumulated rotation vector is related to the autorotation number $m(s_0)$ of the curve:

$$\int_{s_0}^{L+s_0} \boldsymbol{\omega}_A(s_0, s) \cdot \mathbf{D}(s) ds = 2\pi m(s_0) \text{ where } m(s_0) \in \mathbb{Z} \ . \tag{26}$$

For the case that the curve is $\mathcal{C}^3$, and that the frame considered is a Frenet Serret frame (curvature zero not allowed), or a ribbon frame (curvature zero allowed), the vector $\mathbf{D}(s)$ becomes the classical Darboux vector, and the integral in Equation (26) can be written as:

$$\int_{s_0}^{L+s_0} \sqrt{\kappa^2(s) + \tau^2(s)}\, \boldsymbol{\omega}_A(s_0, s) \cdot \mathbf{d}(s)\, ds = 2\pi m(s_0) \text{ where } m \in \mathbb{Z} \ , \tag{27}$$

where $\mathbf{d}$ is a unit vector in the direction of the Darboux vector.

4π instabilities

For a space curve with a closed and smooth frame the derivative $\dot{\phi}(s_0, s)$ of the autorotation can be extended to a periodic function with the period L. This reveals that ϕ has an even number of extrema on the curve interval. Let us look at the case where there are inflection at points s_a and s_b which are also taken to be frame revisit points of s_0, the special case $s_a = s_0$ is allowed. One can simultaneous remove the two inflection points while maintaining a smooth frame. This can be achieved by inverting the sign of the $\mathbf{D}$ vectors in the interval $[s_a, s_b]$. The two curves have autorotations that differ by 0, 4π, or a multiple of 4π, see Figure 3. The two framed curves can be transferred into each other by creating a new set of inflections points between the first set of frame revisit points. In practice, this corresponds to forcing the ribbon to flip around on corresponding part of the ribbon.

Are the autorotation instabilities of relevance for fluid flows?

In this section we briefly discuss some aspects of not just a single framed space curve but of a bundle of framed space curves. As one passes from one space curve to a neighbouring (that may be infinitesimal close) one might encounter an autorotation instability. This means that the infinitesimal volumes defined by the frames will be rotating in manners that are incompatible. It is our thesis that such instabilities are rather common and appear when the autorotation of one curve goes smoothly through a frame revisit point while the neighbouring curve is without a frame revisit point and is therefore forced to rotate towards lower autorotation angles. A special subset of the three-dimensional bundles of framed space curves is the *fluid flows* that are governed by the Navier-Stokes equation and the continuity equation. There is no reason to expect that these fluid flows are exempt from the marks of developing autorotation instabilities and we suggest that such instabilities can offer a generic entry to the phenomenon of turbulence. This is consistent with a delayed onset of turbulence as seen in Reynolds experiments on turbulent pipe flows [44]. Presumably, the frame of the fluid flow first needs to be rotated sufficiently for instabilities to occur as is the case for the autorotation instabilities.

Conclusion

By studying the rotation vector field for a framed space curve we have obtained a detailed relationship between the global rotation vector and the local generalised Darboux vector giving insight into the combination of a global and an incremental rotation. This result is applicable for an arbitrary choice of frame. A condition for having a conserved integral for closed space curves is discussed, and it is shown that instabilities and changes in paths through bifurcations in the autorotation angle can only take place at frame revisit points

if there is a simultaneous shift to, or from, a point where $\sigma_\phi = -1$. This is the reason that the autorotation for closed space curves can change by an integer multiple of 4π as exemplified, e.g. by the Philippine wine dance [45] and the Dirac belt trick [46].

One could wonder if such motions are invoked for specific use within the realm of biology. If so, there would be a resemblance of a double period corresponding to the 4π sequence involved. Two potential candidates in need of further investigations come to our minds. One being the flying snake [47] the other being the question of whether some flights of birds invoke this principle? If one observes carefully the snake, on the co-published video [47], it seems to us that the snake is alternately letting its tail go over and under itself. Thereby it provides a 4π rotation which in principle could be continued indefinitely. The lift is depending on the inclination of the relatively flat side of the snake as discussed in ref. [47]. The motion of the wings of birds is another candidate to be further investigated [48, 49, 50]. Both hovering flight and non-hovering flight. It is necessary to carefully study the direction and orientation of the humerus bone of the wing. Some birds, as the hummingbird, have a relative short humerus bone which can make this inspection difficult. Neither for the case of the flying snake, nor for birds have we yet identified the continuous rotations that should be involved if the mechanism really is driven by 4π increments.

Autorotation instabilities are suggested to be present in 3D patterns of framed flowlines and therefore presumably such instabilities also appear in flows that obey the laws of fluid dynamics. In this case neighbouring infinitesimal fluid volumes would have incompatible rotations at the instabilities and perhaps thus seeding turbulence. Biopolymers is another subject of concern. They undergo important conformational transformations, for example, under helix-coil transitions [51], under the formation or melting of double stranded DNA [52], under the forming of the chromatin fibre [53], and under the folding of proteins [54, 55, 56]. Autorotation instabilities provides a possibility for the releasing of excessive rotations which could help facilitate these processes. These questions are subject to further investigations.

References

[1] Bohr J, Olsen KW.
2013 Total positive curvature of circular DNA.
Phys. Rev. E **88** 052714.
doi:10.1103/PhysRevE.88.052714

[2] Weller C, Nicholson PW, Dobbs SM, Bowes SG, Purkiss A, Dobbs RJ.
1992 Reduced axial rotation in the spouses of sufferers from clinical idiopathic parkinsonism.
Age and Ageing **21**, 189–194.
doi:10.1093/ageing/21.3.189

[3] Pickover AP.
2009 The math book: From Pythagoras to the 57th dimension, 250 milestones in the history of mathematics.
Sterling Publishing Company, New York. ISBN 978-1-4027-5796-9.

[4] Kauffman LH.
2013 *Knots and Physics.*
Vol. 53 World Scientific Publishing Company, Singapore.

[5] Kauffman LH.
1990 An Invariant of regular Isotopy.
Transactions of the American Mathematical Society **318**, 417–471.
doi:10.1090/S0002-9947-1990-0958895-7

[6] Colberg E.
2012 A brief history of knot theory.
Google Scholar Link: www.math.ucla.edu/˜radko/191.1.05w/erin.pdf
Hyperlink

[7] Ricca RL, Nipoti B.
2011 Gauss' linking number revisited
Journal of Knot Theory and its Ramifications **20** 1325-1343.
doi:10.1142/S0218216511009261

[8] Serret JA.
1851 Sur quelques formules relatives à la theéorie des courbes à double courbure.
Journal de Mathématiques pures et appliquées **16** 193–207.
Hyperlink

[9] Frenet F.
1852 Sur les courbes à double courbure.
Journal de Mathématiques pures et appliquées **17** 437–447.
Hyperlink

[10] Bohr J, Markvorsen S.
2013 Ribbon Crystals.
PLoS ONE **8** e74932.
doi:10.1371/journal.pone.0074932

[11] Călugăreanu G.
1961 Sur les classes d'isotopie des noeuds tridimensionnels et leurs invariants.
Czech. Math. J. **11**, 588-625.
Hyperlink

[12] White JH.
1969 Self-linking and the Gauss integral in higher dimensions.
A. J. Math. **91**, 693-728.
doi:10.2307/2373348

[13] Pohl WF.
1968 The self-linking number of a closed space curve.
Indiana Univ. Math. J. **17**, 975-85.
doi:10.1512/iumj.1968.17.17060

[14] Fuller FB.
1971 The writhing number of a space curve.
Proc. Nat. Acad, Sci. USA **68**, 815–819.
Hyperlink

[15] Moffatt HK, Ricca RL.
1992 Helicity and the Călugăreanu invariant.
Proc. R. Soc. Lond. A. **439**, 411-429.
doi:10.1098/rspa.1992.0159

[16] Dias MA, Audoly B.
2015 "Wunderlich meet kirchhoff": A general and unified description of elastic ribbons and thin rods.
Journal of Elasticity **119**, 49-66.
doi:10.1007/s10659-014-9487-0

[17] Felippa CA, Haugen B.
2005 A unified formulation of small-strain corotational finite elements: I. Theory.
Computer Methods in Applied Mechanics and Engineering **194**, 2285–2335.
(doi:10.1016/j.cma.2004.07.035)

[18] Spring KW.
1986 Euler parameters and the use of quaternion algebra in the manipulation of finite rotations: A review.
Machine and Machine Theory **21**, pp. 365–373.
doi:10.1016/0094-114X(86)90084-4

[19] Rodrigues Õ.
1840 Des lois geómétriques qui reǵissent les déplacements d'un systéme solide dans

l'espace, et la variation des coordonnes provenant de ses déplacements considérés indépendamment des causes qui peuvent les produire.
J. Math. Pures Appl., 5 (1840), pp. 380–440.

[20] Gallier J.
2011 Geometric methods and applications for computer science and engineering.
Texts in applied mathematics, Springer, New York. ISBN 978-1-4419-9960-3.

[21] Engø K.
2001 On the BCH-formula in so(3).
BIT Numerical Mathematics **41**, 629–632.
http://dx.doi.org/10.1023/A%3A1021979515229

[22] Gilmore R.
1974 Baker-Campbell-Hausdorff formulas.
Journal of mathematical Physics **15**, 2090-2092.
doi:10.1063/1.1666587

[23] Campbell JE.
1898 On a law of combination of operators.
Proc. Lond. Math. Soc: **29**, 14–32.
Hyperlink

[24] Kauffman LH.
2004 Non-commutative worlds.
New Journal of Physics **6**, 173.
doi:10.1088/1367-2630/6/1/173

[25] Rackovsky S, Scheraga HA.
1978 Differential geometry and polymer conformation. 1. Comparison of protein conformations.
Macromolecules **11**, 1168–1174.
doi:10.1021/ma60066a020

[26] Rappaport SM, Rabin Y.
2007 Differential geometry of polymer models: worm-like chains, ribbons and Fourier knots.
J. Phys. A: math. Theor. **40**, 4455–4466.
doi:10.1088/1751-8113/40/17/003

[27] Kholodenko AL, Vilgis TA.
1998 Some geometrical and topological problems in polymer physics.
Physics Reports **298**, 251-370.
doi:10.1016/S0370-1573(97)00081-1

[28] Hartl J.
1993 Integration of Frenet equations in the isotropic space $I_3^{(1)} = P_{12|000}^3$ by means of quadratures.
Note di Matematica **XIII**, 33–39.
doi:10.1285/i15900932v13n1p33

[29] Hanson AJ, Ma H.
1994 Visualizing flow with quaternion frames.
Proceedings of the conference on Visualization 94,
IEEE, ISBN:0-7803-2521-4 (1994), 108–115.
Hyperlink

[30] Chen BY.
2003 When does the position vector of a space curve always lie in its rectifying plane.
The American Mathematical Monthly **110**, 147-152.
doi:10.2307/3647775

[31] W. Wang W, Jüttler B, Zheng D, Liu Y.
2008 Computation of rotation minimizing frames.
ACM Transactions on Graphics **27**, 2.
doi:10.1145/1330511.1330513

[32] Farouki RT, Han CY.
2003 Rational approximation schemes for rotation-minimizing frames on Pythagorean-hodograph curves.
Computer Aided Geometric Design **20**, 435-454.
doi:10.1016/S0167-8396(03)00095-5

[33] Karacan MK, Bükcü B.
2010 On natural curvatures of Bishop frame.
Journal of Vectorial Relativity **5**, 34–41.

[34] Dandoloff R, Zakrzewski WJ.
1989 Parallel transport along a space curve and related phases.
Journal of Physics A: Mathematical and Theoretical **22**, L461–L466.
doi:10.1088/0305-4470/22/11/003

[35] Horn BKP.
1987 Closed-form solution of absolute orientation using unit quaternions.
Journal of the Optical Society of America A **4** pp. 629–642.
doi:10.1364/JOSAA.4.000629

[36] Cheng-Chung H.
1981 A differential-geometric criterion for a space curve to be closed.

Proceedings of the American Mathematical Society **83**, 357–361.
doi:10.2307/2043528

[37] Nomizu K.
1959 On Frenet equations for curves of class $\mathbf{C}^\infty$.
Tohoku Math. J. **11**, 106-112,
doi:10.2748/tmj/1178244631

[38] Bates LM, Melko OM.
2013 On curves of constant torsion I.
J. Geom. **104**, 213-227.
doi:10.1007/s00022-013-0166-2

[39] Randrup T, Røgen P.
1996 Sides of the Möbius strip.
Arch. Math. **66**, 511-521.
doi:10.1007/BF01268871

[40] Starostin EL, van der Heijden GHM.
2007 The shape of a Möbius strip.
Nature Materials **6**, 563–567.
doi:10.1038/nmat1929

[41] Giomi L, Mahadevan L.
2010 Statistical Mechanics of developable ribbons.
Phys. Rev. Lett. **104**, 238104.
doi:10.1103/PhysRevLett.104.238104

[42] Starostin EL, van der Heijden GHM.
2011 Comment on "Statistical mechanics of developable ribbons".
Phys. Rev. Lett. **107**, 239801.
doi:10.1103/PhysRevLett.107.239801

[43] Ricca RL.
2005 Inflexional disequilibrium of magnetic flux-tubes.
Fluid Dynamics Research **36**, 319-332.
doi:10.1016/j.fluiddyn.2004.09.004

[44] Lautrup L.
2011 Physics of Continuous Matter, Exotic and Everyday Phenomena in the Macroscopic World, Second Edition.
CRC Press, New York.

[45] Feynman RP, Weinberg S.
2011 The 1986 Dirac memorial lecture.
in *Elementary particles and the laws of physics*,
Cambridge University Press, 13th printing, Cambridge.

[46] Staley M.
2010 Understanding quaternions and the Dirac belt trick.
European Journal of Physics **31**, 467–478.
doi:10.1088/0143-0807/31/3/004

[47] Holden D, Socha JJ, Cardwell DN, Pavios P.
2014 Aerodynamics of the flying snake Chrysopelea paradisi: how a bluff body cross-sectional shape contributes to gliding performance.
Journal of Experimental Biology **217**, 382–394.
doi:10.1242/jeb.090902

[48] Warrick DR, Tobalske BW, Powers DR.
2005 Aerodynamics of the hovering hummingbird.
Nature **435**, 1094-1097.
doi:10.1038/nature03647

[49] Tobalske BW.
2007 Biomechanics of bird flight.
Journal of Experimental Biology **210**, 3135-3146.
doi:10.1242/jeb.000273

[50] Hedrick TL, Tobalske BW, Ros IG, Warrick DR, Biewener AA.
2011 Morphological and kinematic basis of the hummingbird flight stroke: scaling of flight muscle transmission ratio.
Proceedings of the Royal Society of London B: Biological Sciences rspb20112238.
doi:10.1098/rspb.2011.2238

[51] Badasyan A, Tonoyan SA, Giacometti A, Podgornik R. Parsegian VA, Masakhlisov YS, Morozov VF.
2014 Unified description of solvent effects in the helix-coil transition.
Phys. Rev. E **89**, 022723.
doi:10.1103/PhysRevE.89.022723

[52] Marie R, Pedersen JN, Bauer DLV, Rasmussen KH, Yusuf M, Volpi E, Flyvbjerg H, Kristensen A, Mir KU.
2013 Integrated view of genome structure and sequence of a single DNA molecule in nanofluidic device.
Proceedings of the National Academy of Science **110**, 4893-4898.
doi:10.1073/pnas.1214570110

[53] Barbi M, Mozziconacci J, Victor JM, Wong H, Lavelle C.
2012 On the topology of chromatin fibres.
Interface Focus **2**, 546-554.
doi:10.1098/rsfs.2011.0101

[54] Anfinsen CB.
1973 Principles that govern the folding of protein chains.
Science **181**, 223-230.
doi:10.1126/science.181.4096.223

[55] Rose GD, Fleming PJ., Banavar JR, Maritan A.
2006 A backbone-based theory of protein folding.
Proceedings of the National Academy of Science **103**, 16623-16633.
doi:10.1073/pnas.0606843

[56] Dill KA, Ozkan SB, Weikl TR, Chodera JD, Voelz VA.
2007 The protein folding problem: when will it be solved?
Current Opinion in Structural Biology **17**, 342-346.
doi:10.1016/j.sbi.2007.06.001

Figures and Figure Captions:

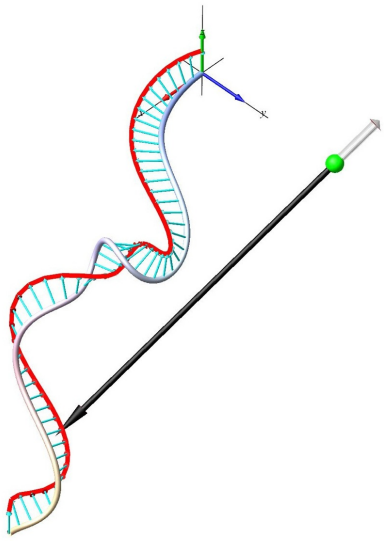

Figure 1: An example of autorotation. The framed curve starts at the origin of the coordinate system. The space curve is shown as a grey tube, and the first frame vector, $\mathbf{e}$, is along its tangent. The second frame vector, $\mathbf{g}$, is depicted as the turquoise unit vector ending at the red curve. The autorotation vector, $\mathbf{\Omega}_A$, from the beginning of the curve to the end is given by the black vector. The corresponding autorotation angle ϕ_A is -2π, and the corresponding unit field vector $\boldsymbol{\omega}_A$ is depicted as the white unit vector at the green dot.

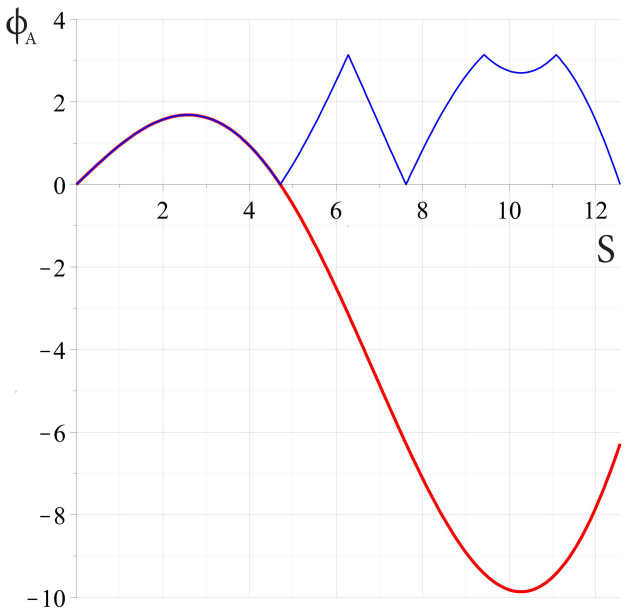

Figure 2: The red curve shows the autorotation angle, $\phi_A(s)$, as a function of the curve-length, s, for the framed space curve depicted in Figure 1. The blue curve show the corresponding angle $\phi_{2p} \in [0, \pi]$ discussed in Equation 1.

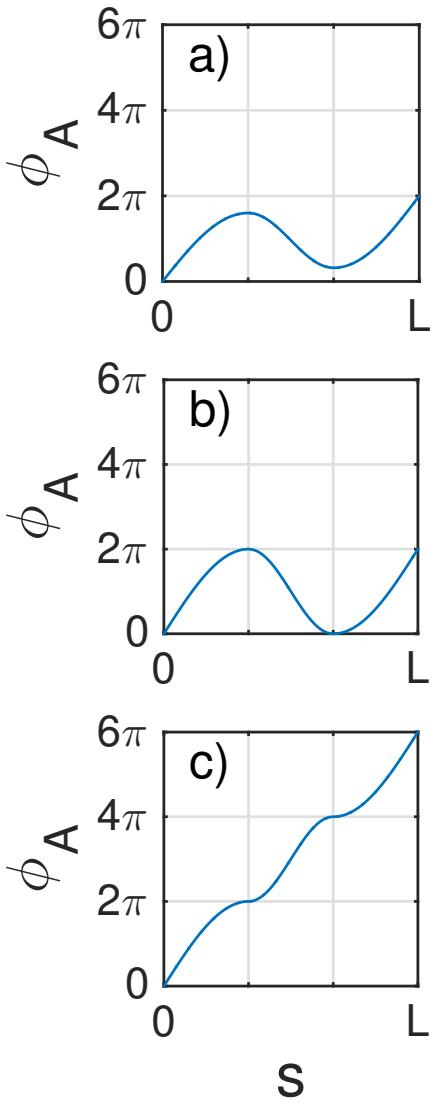

Figure 3: Schematic depiction of the autorotation angle ϕ_A. a) A case with two extrema and no frame revisit points. b) Here there are two extrema which are also frame revisit points. c) After a global reconfiguration of the extrema of the autorotation $\phi(L)$ has grown by 4π.